Research Article

The Gold Nanoparticles Functionalized with the Synthetic PADRE^S2P6 Peptide Can Be Useful for SARS-CoV-2 Detection

Charline Herrscher[1], Maroua Ben Haddada[2], Jessica Andries[1], Wildriss Viranaicken[1], Colette Cordonin[3], Gilles Gadea[1†], Patrick Mavingui[1], Chaker El-Kalamouni[1], Anne-Laure Morel[2], Philippe Desprès[1*]

[1]Université de la Réunion, INSERM U1187, CNRS UMR 9192, IRD UMR 249, Unité Mixte Processus Infectieux en Milieu Insulaire Tropical (PIMIT), Plateforme Technologique CYROI, 2 rue Maxime Rivière, 97490 Sainte Clotilde, La Réunion, France
[2]TORSKAL Nanoscience, Plateforme Technologique CYROI, 2 rue Maxime Rivière, 97490 Sainte Clotilde, La Réunion, France
[3]Plateforme Technologique CYROI, 2 rue Maxime Rivière, 97490 Sainte Clotilde, La Réunion, France
E-mail: philippe.despres@univ-reunion.fr
[†]Present Address: IRCM, U1194, MetaSarc team, 34298 Montpellier, France

Abstract: Conjugation of bioactive peptides to nanomaterials is a promising approach for a variety of biomedical uses. Indeed, we assumed that gold nanoparticles (AuNPs) functionalized with synthetic viral peptides represent a promising strategy to elicit antibody response against zoonotic coronavirus SARS-CoV-2 responsible for pandemic COVID-19 disease. Two specific linear B-cell epitopes namely S1P4 and S2P6 have been recently identified in the SARS-CoV-2 spike protein expressed by the COVID-19 mRNA BNT162 vaccine of Pfizer-BioNTech and marketed under the brand name Comirnaty. The present study aimed at investigating the immunogenic potential of AuNPs functionalized with synthetic PADRE^S1P4 and PADRE^S2P6 peptides in a mouse model. The AuNPs were synthesized using an environmentally friendly process. In both synthetic PADRE^S1P4 and PADRE^S2P6 peptides, the SARS-CoV-2 spike antibody epitope is preceded by a polybasic sequence and the T-helper cell response activator PADRE. A thiol-terminated polyethylene glycol was used to decorate AuNP surface with the synthetic peptides. The AuNPs-peptide conjugates were inoculated without any adjuvant to adult BALB/c mice by intramuscular route in a prime-boost schedule. The AuNPs functionalized with the PADRE^S2P6 peptide but not the PADRE^S1P4 peptide were efficient to elicit antibody production of relevant specificity against the SARS-CoV-2 spike protein. The ability of PADRE^S2P6 peptide-reactive antibodies to recognize SARS-CoV-2 variants opens important perspectives for AuNP-peptide conjugates as potential serological tools to support the surveillance of wildlife-origin coronaviruses.

Keywords: gold nanoparticles; coronavirus; COVID-19; SARS-CoV-2; spike protein; linear B-cell epitope; synthetic peptide; antibodies

1. Introduction

The recent years are deeply marked by outbreaks of emerging and re-emerging pathogens from wildlife reservoirs spilling over to human population [1]. The recently emerged Coronavirus disease 2019 (COVID-19) is a remarkable

example of pandemic infectious disease leading to a significant impact on public health with an estimated 15 million excess deaths for the period 2020-2021 [2, 3]. The COVID-19 pandemic shed light on the urgent need to develop new strategies for detecting, preventing and treating wildlife-origin coronaviruses with high epidemic potential. Nanomedicines have demonstrated their usefulness in vaccine platforms and nanoparticle-encapsulated COVID-19 mRNA vaccines marketed as Comirnaty (BNT162 vaccine under license from Pfizer/BioNTech) and Spikevax (under license from Moderna) have greatly contributed to the fight against SARS-CoV-2, the etiologic agent of COVID-19. We recently reported that individuals who had received COVID-19 mRNA Comirnaty vaccine developed antibodies recognizing two linear B-cell epitopes, namely S1P4 and S2P6, located in the spike protein of SARS-CoV-2 [4]. There was a lack of reactivity of S1P4 and S2P6 antibody epitopes with immune sera from COVID-19 recovered patients suggesting that their immune recognition would be an antigenic property of recombinant spike protein expressed by Comirnaty vaccine [4]. SARS-CoV-2 spike protein is structurally divided into S1 and S2 subunits [2]. The S1 subunit (residues 1/685) contains the receptor-binding domain of SARS-CoV-2. After virus binding to cell surface, the released S2 subunit (residues 686/1273) catalyzes fusion between the viral and host-cell membranes. S1P4 antibody epitope (residues S-616 to S-644) localizes to the C-terminal region of S1 subunit whereas S2P6 antibody epitope (residues S-1138 to S-1169) is found downstream of the transmembrane domain of S2 subunit. So far, the two antibody epitope sequences are strictly conserved among recent SARS-CoV-2 Variants of Concern (VOC) including Omicron [4].

Recently, nanoparticles have benefited from the necessity to develop new strategies against emerging pathogens taking advantage of their efficiency as vaccine platforms [5–8]. Here, we were interested in using nanomaterials for development of SARS-CoV-2 detection tools, inert nanoparticles been able to cross blood and tissues barriers [9, 10]. The multivalent binding capacity of gold nanoparticles (AuNPs) makes them attractive candidates as nanoscale-sized biocompatible carriers for conjugation with bioactive peptides. However, nanoparticle-cell interactions could trigger oxidative stress and inflammatory cytokine cascade activation once AuNPs have been incorporated into the cell via the endocytic pathway [11]. To prevent such effects, the current researches have focused on the development of innovative manufacturing processes to reduce AuNP toxicity such as environmental-friendly approaches [12, 13].

We recently reported that peptide-reactive antibodies were detected in mice immunized with the synthetic S2P6 peptide, and to a lesser extent the synthetic S1P4 peptide, coupled to protein carrier keyhole limpet hemocyanin (KLH) [4]. The present study aimed at investigating the ability of AuNPs to bioconjugate with two SARS-CoV-2 spike epitope peptides, as well as to trigger an humoral response against the AuNP-peptide conjugates in a mouse model. For this purpose, AuNPs were synthesized using a green chemistry-based process and then functionalized with synthetic peptides designed as PADRE^S1P4 and PADRE^S2P6. The immunogenicity of AuNP-peptide conjugates was evaluated in BALB/cJRj mice. We showed that AuNP-PADRE^S2P6 peptide conjugates have ability to elicit antibody production of relevant specificity against SARS-CoV-2 spike protein.

2. Materials and methods

2.1 Cells, viruses and antibodies

Human lung epithelial A549[ACE2+, TMPRSS2+] cell line overexpressing human ACE2 and TMPRSS2 proteins was purchased from Invivogen (Toulouse, France). A549[ACE2+, TMPRSS2+] cells, human epithelial HEK-293T cells and human hepatoma Huh 7.5 cells were grown in Dulbecco's modified Eagle's medium (DMEM) growth medium supplemented with heat-inactivated 10% fetal calf serum and antibiotics. A549[ACE2+, TMPRSS2+] cells were infected with La Réunion 2020 SARS-CoV-2 isolate at the multiplicity of infection 0.001. Huh 7.5 cells were infected with HCoV-229E virus (a generous gift of V. Thiel, University of Zürich and K. Séron, Institut Pasteur Lille) at the multiplicity of infection 0.2. Anti-SARS-CoV-2 spike antibody covrbdc2-mab1 was obtained from Invivogen (Toulouse, France). Anti-dsRNA antibody J2 obtained from Abcam (Paris, France) was used to detect HCoV-229E virus. Rabbit anti-FLAG antibody obtained from DIAGNOMICS (Blagnac, France) was used to detect recombinant SARS-CoV-2 spike protein. Donkey IgG anti-rabbit IgG-Alexa Fluor 488, anti-mouse IgG-Alexa Fluor 594 and anti-human IgG-Alexa Fluor 594 obtained from Thermo Fisher Scientific (Les Ulis, France) were used as secondary antibodies for IF analysis.

2.2 Recombinant SARS-COV-2 spike protein

Mammalian codon-optimized gene coding for a soluble spike protein (residues 1 to 1195) from Omicron variant SARS-CoV-2 (Genbank access UJE45220.1) was established using *Homo sapiens* codon usage as reference. A sequence encoding the GCN4-IZ trimerization domain followed by a glycine-serine spacer and a FLAG tag was inserted in frame at the C-terminus of recombinant soluble spike protein (rS). The residue substitutions at positions S-986 and S-987 with two proline led to a prefusion stabilized rS protein. The residue substitutions at positions S-682, S-S683, and S-685 with three alanine led to remove the furin-like cleavage site at the S1/S1 subunit boundary. The synthesis of gene sequence and their cloning into *Nhe-I* and *Not-I* restriction sites of the pcDNA3.1 Hygro (+) vector plasmid to generate recombinant pcDNA3/rS were performed by Genecust ((Boynes, France). The plasmid sequence was verified by Sanger method. HEK-293T cells were transiently transfected with pcDNA3/rS^{Omicron} using Lipofectamine 3,000 (Thermo Fosher Scientific, les Ulis, France).

2.3 Conjugation of synthetic peptide to AuNPs

All the synthetic peptides were chemically synthetized by Genecust (Boynes, France). The peptides were dissolved in DMSO and then diluted in sterile H_2O as previously described [4]. AuNPs were synthesized by a green method as previously described [12]. To determine the optimal peptide concentration for binding to AuNPs, the colloids were mixed with increasing peptide concentrations from 0.06 to 32 µM for 2 h at room temperature. To check the completeness of the peptide conjugation, equal volume of 10% NaCl was added 24 h later and UV-Vis spectrum of the mixture was measured [14]. Once optimal peptide concentration was defined, the bioconjugation reaction was scaled up and the colloidal solution was freed from excess free peptide by centrifugation at 10,000 g for 20 min at 4 °C. The pellet of peptide-AuNPs conjugates was resuspended in PBS and the particle size in colloidal solution was measured by Dynamic Light Scattering (DLS) method using a Zetasizer Nano ZS (Malvern Instruments, Malvern, UK) at 25 °C. The measurements were made in triplicate. The theoretical optimal peptide-AuNP ratio (Rpeptide/AuNP) in peptide. com-2 was obtained by calculating the ratio between the AuNP surface (S_{AuNP}), the AuNP concentration (C_{AuNP}), and the peptide concentration ($C_{peptide}$) as follows: Rpeptide/AuNP = SAuNP $\times$ [$C_{peptide}/C_{AuNP}$]. For further experiments, the nanoconjugates was stored at 4 °C in PBS supplemented with 0.01% Tween-20. For animal experiments, the AuNP-peptide conjugates were twice washed with PBS and then stored in cold sterile PBS.

2.4 Mouse experiment and ethical statement

Groups of five 6-week-old female BALB/cJRj mice (Janvier Labs, France) were inoculated with AuNP-PADRE^S1P4 or AuNP-PADRE^S2P6 conjugates in 0.1 mL sterile PBS by intramuscular (i.m.) route over two injection sites. Mice that received 5 µg of AuNP-peptide conjugates were boosted with the same dose two weeks after the prime dose. Retro-orbital blood sampling was performed on anesthetized mice two weeks after the first boost. A third dose of AuNP-peptide conjugates was inoculated one month after the antigenic boost. One month after the second boost, blood sampling was performed on anesthetized mice. All animals were daily observed to detect any stress or suffering. No morbidity was observed in mice that received colloidal solution by i.m. route. As an immunogenic control, adult BALB/cJRj mice were inoculated with synthetic S2P6 peptide conjugated to protein carrier keyhole limpet hemocyanin (KLH) in complete Freund's adjuvant by i.m. route. Mice that received 20 µg of KLH-peptide conjugates were boosted three times after primary immunization. One month after the last immunization, blood sampling was performed on anesthetized mice. The Animal Ethics Committee of CYROI No. 114 approved all the animal experiments with reference APAFIS#32599-2021060109058958v2 (July 2021). The animal procedures were performed in accordance with the European Union legislation for the protection of animals used for scientific purposes (Directive 2010/63/EU). The study was conducted following the guidelines of the Office Laboratory of Animal Care (agreement No. 974 001 A) at the Cyclotron and Biomedical Research CYROI platform, Sainte-Clotilde, La Reunion, France and in accordance with the ARRIVE guidelines (https://arriveguidelines. org).

2.5 Peptide-based ELISA method

The peptide-based ELISA tests were essentially performed as previously described [4]. Briefly, a 96-well plate was coated with 0.1 mL of synthetic S1P4, S2P6 or S2P6.2.0 peptide at final concentration of 0.2 µg·mL^{-1} at 4 °C overnight. The wells were incubated with mouse serum sample at 37 °C for 2 h and then anti-mouse IgG HRP-conjugated secondary antibody at final dilution 1:2000 at room temperature for 1 h. The wells were incubated with TMB substrate solution at room temperature for 3 min. Absorbance was measured using microplate reader at 450 nm.

2.6 Immunoblot assay

The immunoblot assay was essentially performed as previously described (4). Briefly, cells were lysed in RIPA lysis buffer (Sigma, Lyon, France). Proteins were separated by SDS-PAGE and transferred into a nitrocellulose membrane. Blots were incubated with mouse immune serum at dilution 1:200 and then anti-mouse IgG HRP-conjugated secondary antibody. The membranes were revealed with ECL detection reagent (Thermo Fisher Scientific, Les Ulis, France) and exposed on an Amersham imager 680 (GE Heathcare).

2.7 Immunofluorescence assay

Cells grown on coverslips were fixed with 3.7% paraformaldehyde for 20 min and then permeabilized with 0.1% Triton X-100 in PBS for 4 min. Cells were stained with mouse immune serum at dilution 1:100 and the incubated by anti-mouse Alexa Fluor 488 IgG secondary antibody. The nucleus was stained with DAPI. Cells were visualized with a Nickon Eclipse E-2000-U microscope (Nikon, Lisses, France).

2.8 Statistical analysis

Paired t tests were used to compare quantitative data. GraphPad Prism 9 was used for all statistical analysis.

3. Results

3.1 Functionalization of AuNPs with synthetic peptides

The AuNPs were synthesized using a green chemistry method [12] and then functionalized with the synthetic peptides PADRE^S1P4 and PADRE^S2P6 (Table 1). The two peptides include the SARS-CoV-2 B-cell epitopes corresponding to spike residues 616/644 in the S1 subunit or 1138/1169 in the S2 subunit, respectively [4]. The viral peptide sequences are preceded by the *pan* HLA-DR reactive epitope AKFVAAWTLKAAA (PADRE) acting as T-helper cell response activator in humans. Between PADRE sequence and viral peptides is a dibasic peptide. The N-terminal part of both PADRE^S1P4 and PADRE^S2P6 peptides is made of the polybasic sequence RARKRR. Following internalization of AuNP-peptide conjugates into the cytoplasm, the RARKRR sequence at the AuNP surface-peptide junction can be subjected to a proteolytic cleavage releasing the immobilized peptides from the nanoparticle surface. Conjugation of PADRE^S1P4 and PADRE^S2P6 peptides with AuNPs was achieved by PEGylation of the two peptides with SH-CH$_2$-CH$_2$-CO-(PEG)$_5$ polymer (designed hereafter as SH-PEG) linked to the N-terminal arginine of the peptide (Table 1). The peptide binding to the gold surface was accomplished via the free sulfhydryl group of SH-PEG compound. A cysteine residue has been identified at position 23 of the PADRE^S1P4 peptide (Table 1). It is not known whether the free thiol group of Cys23 has ability to interact with the surface of AuNPs.

Table 1. Synthetic peptide sequences

Peptide	Amino acid sequence	Size
PADRE^S1P4*	RARKRRAKFVAAARR<u>NCTEVPVAIHADQLTPTWRVYSTGSNVFQ</u>	51-mer
PADRE^S2P6**	RARKRRAKFVAAARR<u>YDPLQPELDSFKEELDKYFKNHTSPDVDLGDI</u>	54-mer

*   The S1P4 antibody epitope is underlined.
** The S2P6 antibody epitope is underlined.

The 15 nm-sized AuNPs, whose advantages include biocompatibility, high surface to volume ratio, and cell internalization [12, 14] were functionalized with increasing concentrations of synthetic PADRE^S1P4 or PADRE^S2P6 peptide to generate AuNP-PADRE^S1P4 and AuNP-PADRE^S2P6 peptide conjugates, respectively. The conjugation was monitored by Localized Surface Plasmon Resonance (LSPR) band as indicator for colloidal stability [14, 15]. A redshift from original colloid spectrum (i.e., non-functionalized AuNPs) was observed at micromolar concentrations of synthetic peptides conjugated to 1 O.D. unit of AuNPs (Figure 1A). A flocculation test in the presence of high salt concentrations indicated that optimal concentrations for peptide conjugation were 2 or 4 µM for the synthetic PADRE^S1P4 peptide and PADRE^S2P6 peptide, respectively (Figure 1B).
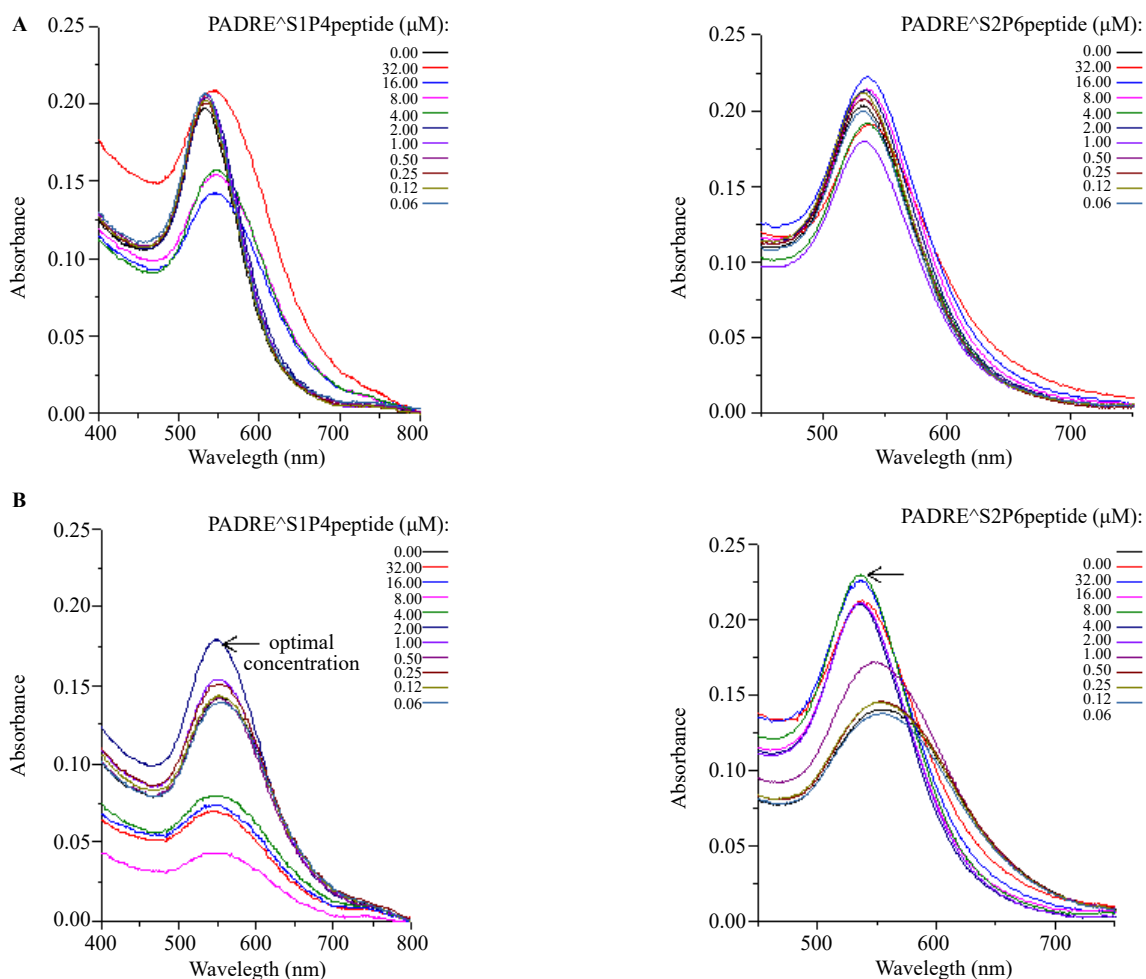

Figure 1. Functionalization of AuNP-peptide conjugates characterized by LSPR. AuNPs were mixed 2 h with increasing concentrations of the synthetic PADRE^S1P4 or PADRE^S2P6 peptide. *In* (**A**), AuNP-peptide conjugates conjugates were examined by LSPR with an extended spectral range. *In* (**B**), flocculation tests on AuNP-peptide conjugates were performed in presence of 10% NaCl for 24 h. The optimal concentrations of peptide are indicated.

By LSPR method, we observed that conjugation of 2 μM synthetic PADRE^S1P4 peptide or 4 μM synthetic PADRE^S2P6 peptide to AuNPs resulted in a similar 5 nm shift as compared to non-functionalized AuNPs (Figure 2). The conjugation of the two peptides onto 15 nm-sized AuNPs gave a theoretical peptide-gold nanoparticle surface ratio of about 10^{15}. The measures of AuNP-peptide conjugates by DLS method showed an increase in their hydrodynamic diameter from 58.1 ± 1.3 to 65.3 ± 5.2 nm without any aggregation. These conditions were considered as optimal and used for further experiments. The two lots of AuNP-peptide conjugates were stored in sterile DPBS at 4 °C.
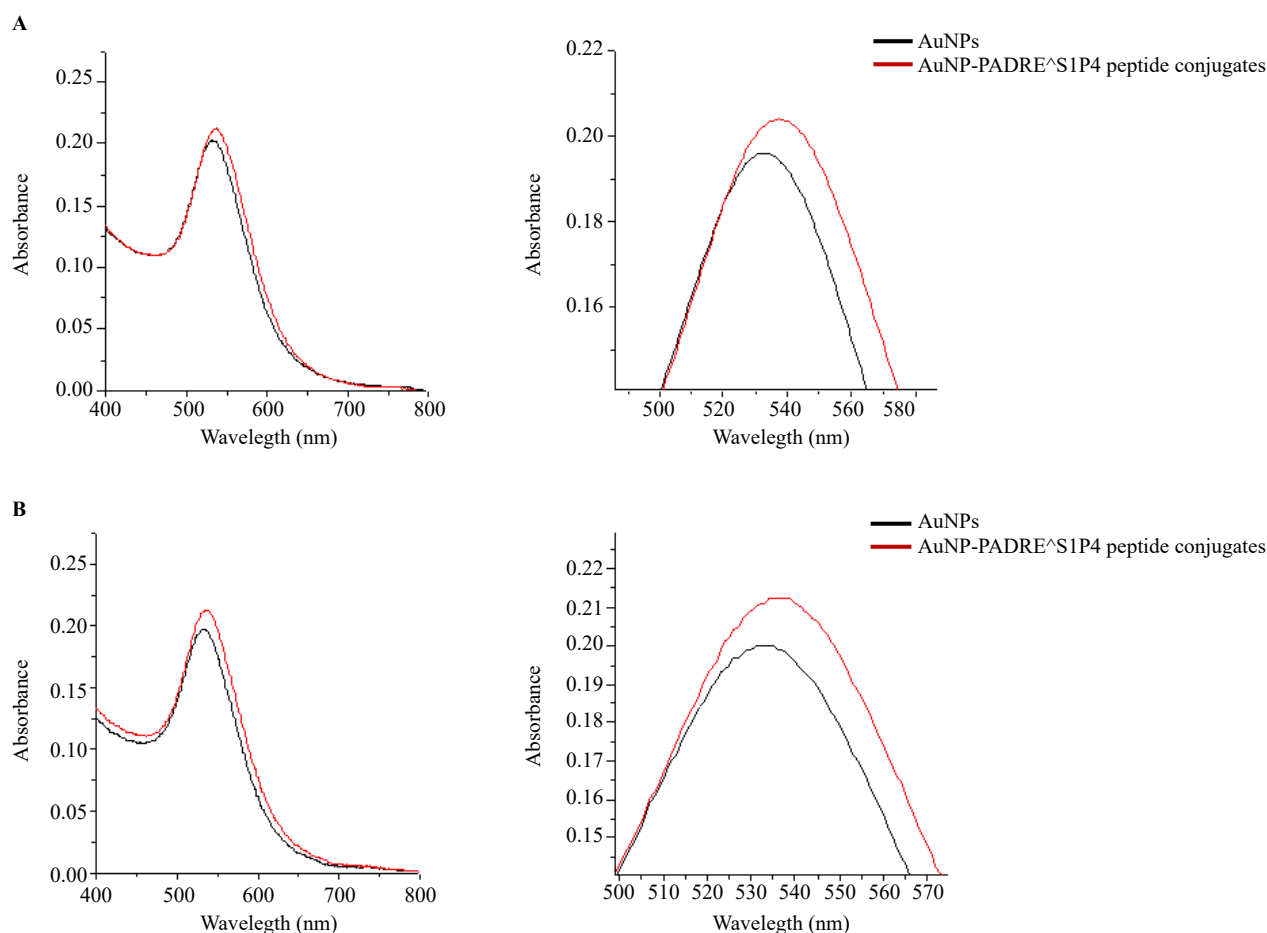

Figure 2. Functionalization of AuNP-peptide conjugates analyzed by UV/Vis spectroscopy. AuNPs functionalized with 2 μM synthetic PADRE^S1P4 peptide (AuNP-PADRE^S1P4 peptide conjugates) (**A**) or 4 μM synthetic PADRE^S2P6 peptide (AuNP-PADRE^S2P6 peptide conjugates) (**B**) were analyzed by UV/Vis spectroscopy with an extended spectral range (left) or a focus on 500/600 nm (right). The profiles of AuNP-peptide conjugates and free AuNPs were compared.

3.2 *Antibody response against AuNP-peptide conjugates*

Adult BALB/c mice were intramuscularly immunized with 5 μg AuNP-PADRE^S1P4 peptide or AuNP-PADRE^S2P6 peptide conjugates in phosphate-buffered saline (PBS) via needle injection route and without any adjuvant. Animals received booster inoculations with the same doses two and then six weeks after the prime dose. Control animals were injected with AuNPs diluted in PBS or PBS alone. Repeated administrations of AuNPs or AuNP-peptide conjugates caused no obvious adverse events relating to body weight and behavioural change on study period. Mice were bled two weeks after the first antigenic boost and four weeks after the second one for serological analysis. Individual mouse immune sera were tested on synthetic S1P4 or S2P6 peptide through a peptide-based ELISA [4].

Serum samples from mice that received AuNP-PADRE^S1P4 peptide conjugates showed no immune reactivity

with the synthetic S1P4 peptide (Figure 3A). Thus, AuNPs functionalized with synthetic PADRE^S1P4 were inefficient to elicit specific antibody response in BALB/c mice inoculated by i.m. route in a prime-boost schedule
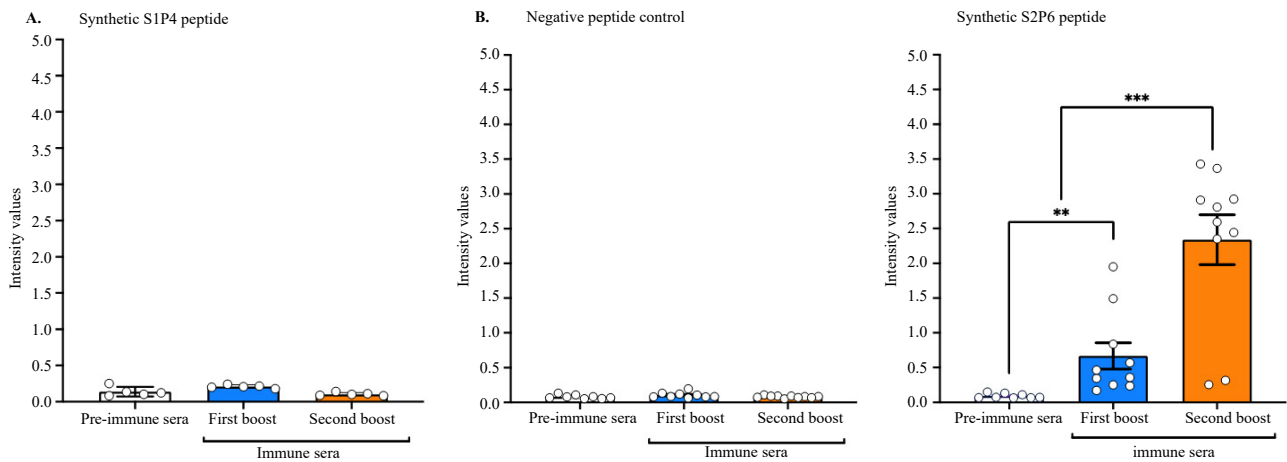

Figure 3. Antibody response against AuNP-peptide conjugates. *In* (**A**), serum samples from mice that received AuNP-PADRE^S1P4 peptide conjugates were collected after the first and second antigenic boost by i.m. route, and assessed by peptide-based ELISA using synthetic S1P4 peptide. The pre-immune mouse sera served as negative serum controls. The intensity values of serum samples at dilution 1:50 were measured at OD_{450}. There were no statistically significant differences between pre-immune sera and immune sera. *In* (**B**), serum samples from mice were collected after the first or second boost of AuNP-PADRE^S2P6 peptide conjugates by i.m. route, and assessed by peptide-based ELISA using the synthetic S2P6 peptide or the synthetic S2P6.2.0 peptide as negative peptide control. The pre-immune mouse sera served as serum controls. The intensity values of serum samples at dilution 1:50 were measured at OD_{450}. Statistically significant differences were observed with the synthetic S2P6 peptide (** $p < 0.01$, *** $p < 0.001$).

Peptide-based ELISA revealed that individual BALB/c mice that received two doses of AuNP-PADRE^S2P6 peptide conjugated developed S2P6-reactive antibodies as compared to pre-immune serum samples (Figure 3B). The synthetic mutant S2P6.2.0 peptide which has been shown not to be efficient for recognition by S2P6 peptide-reactive antibodies was used as a negative control [4] (Figure 3B). The lack of S2P6.2.0 recognition highlighted the ability of AuNP-PADRE^S2P6 peptide conjugates to elicit antibody production of relevant specificity against the SARS-CoV-2 spike protein. Inoculation of AuNP-PADRE^S2P6 peptide conjugates one month after the first boost dose significantly increased immune reactivity of mouse serum against the synthetic S2P6 peptide by peptide-based ELISA (Figure 3B). Among the ten immune sera samples tested, at least eight displayed high S2P6 peptide-reactive antibody titres ranging from 400 to 1,600 with a ISR mean value of 800 (Figure 4). Together, these results showed that adult BALB/c mice i.m. immunized with three doses of AuNP-PADRE^S2P6 peptide conjugates developed specific antibodies with a strong reactivity against SARS-CoV-2 spike protein. In contrast, AuNP-PADRE^S1P4 peptide conjugates were inefficient to elicit specific antibody response.
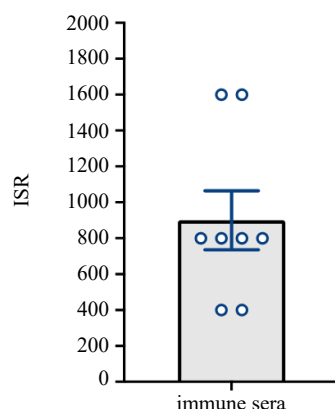
Figure 4. Determination of Immune Status Ratio (ISR) of mice that received AuNP-PADRE^S2P6 peptide conjugates. The eight mouse immune serum samples showing a significant reactivity against the synthetic S2P6 peptide (Figure 3B) were evaluated for their ISR through a peptide-based ELISA. The ISR is calculated from the ratio of the OD_{450} obtained with the synthetic S2P6 peptide divided by OD_{450} obtained with the synthetic S2P6.2.0 peptide that has been used as a negative peptide control. The end-point titer of each sample was calculated as the reciprocal of the last dilution of serum having ISR value > 10.

3.3 Recognition of SARS-CoV-2 spike protein by PADRE^S2P6 peptide-reactive antibody

The reactivity of immune sera from BALB/c mice inoculated with AuNP-PADRE^S2P6 peptide conjugates was assessed on highly permissive A549[ACE2+, TMPRSS2+] cells infected with SARS-CoV-2 isolated in La Reunion in 2020. A mouse serum positive for S2P6 peptide-reactive antibodies with a titer of 800 and its respective pre-immune serum were tested on A549[ACE2+, TMPRSS2+] cells by immunofluorescent assay (IF) (Figure 5A). A monoclonal antibody of relevant specificity against the SARS-CoV-2 spike protein was used as positive antibody control. IF analysis revealed that immune serum at dilution 1:100 but not the pre-immune serum reacts with the intracellular spike protein expressed in A549[ACE2+, TMPRSS2+] cells infected with SARS-CoV-2 (Figure 5A). Then, the ability of AuNP-PADRE^S2P6 peptide conjugates to elicit antibody production of relevant specificity was evaluated in Huh7.5 cells infected with human alphacoronavirus HCoV-229E. IF assay showed no reactivity of immune serum with HCoV-229E spike protein (Figure A1). We also tested the reactivity of immune sera from BALB/c mice that received AuNP-PADRE^S2P6 peptide conjugates on SARS-CoV-2 spike protein by immunoblot assay (Figure 5B). We previously developed mouse S2P6-reactive antibodies against the SARS-CoV-2 spike protein immunizing adult BALB/c mice with KLH-S2P6 peptide conjugates in a prime-boost schedule by i.m. route [4]. A KLH-S2P6 serum sample with S2P6 peptide-reactive antibody titer of 3,200 (Figure A2) was able to detect the spike protein from lysates of A549[ACE2+, TMPRSS2+] cells infected by SARS-CoV-2 (Figure 5B). Immunoblot assay demonstrated that immune serum raised against AuNP-PADRE^S2P6 peptide conjugates at dilution 1:200 can recognize SARS-CoV-2 spike protein and the pattern of antibody reactivity was comparable to that of immune serum from mouse that received KLH-S2P6 peptide conjugates.
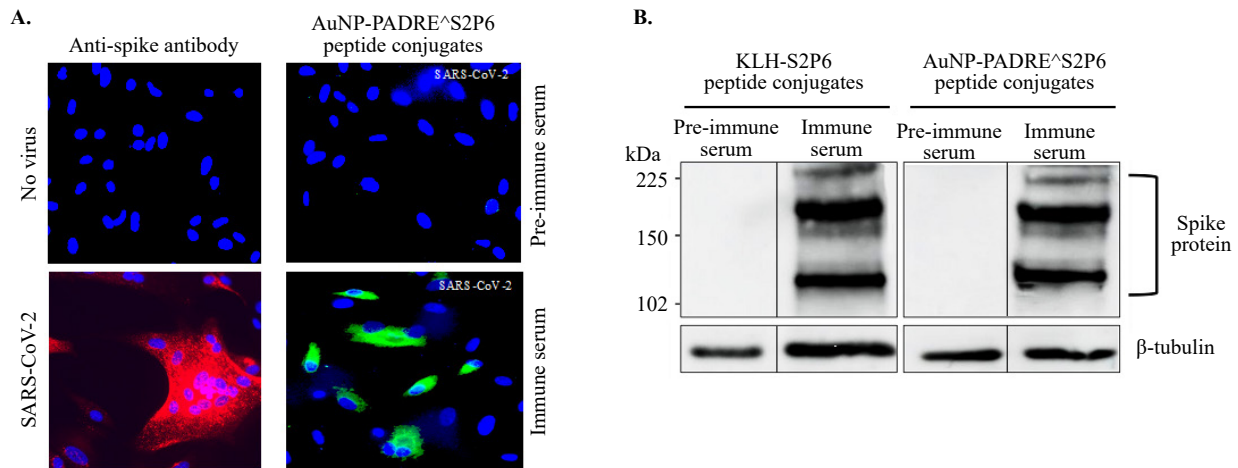
Figure 5. Recognition of SARS-CoV-2 by PADRE^S2P6 peptide-reactive antibody. *In* (A), IF analysis on A549^{ACE2+ TMPRSS2+} cells infected 24 h with SARS-CoV-2 or mock-infected (no virus) was performed using human anti-SARS-CoV-2 spike monoclonal antibody (anti-spike antibody) as positive antibody control, immune serum raised against AuNP-PADRE^S2P6 peptide conjugates (immune serum) or its respective pre-immune serum at dilution 1:100. Donkey IgG anti-human IgG-Alexa Fluor 594 and anti-mouse IgG-Alexa Fluor 488 served as secondary antibody. Nuclei were stained by DAPI. Slides were observed under 20x lens magnification. *In* (B), immunoblot assay on RIPA lysates from A549ACE2+ TMPRSS2+ cells infected 24 h with SARS-CoV-2 using immune serum raised against AuNP-PADRE^S2P6 peptide conjugates and its respective pre-immune mouse serum at dilution 1:200. Mouse immune serum raised against KLH-S2P6 peptide conjugates was used as positive control serum and its respective pre-immune mouse serum served as negative serum control. The SARS-CoV-2 spike protein is indicated. Intracellular ß-tubulin served as protein loading control.

The immune reactivity of serum from mice that received AuNP-PADRE^S2P6 peptide conjugates was next assessed on spike protein from SARS-CoV-2 variant Omicron that has been classified as VOC. For this purpose, codon-optimized gene rS encoding the soluble form of spike protein (residues S-1/1195) from SARS-CoV-2 Omicron variant followed by a trimerization domain and a FLAG tag was inserted into a shuttle plasmid to generate recombinant plasmid pcDNA3/rS. IF assay was performed on HEK-293T cells transfected 24 h with pcDNA3/rS (Figure 6). A rabbit anti-FLAG antibody detected the expression of rS in transfected cells. The immune serum of mouse that received AuNP-PADRE^S2P6 peptide conjugates gave a positive signal on HEK-293T cells expressing rS (Figure 6). Together, these results highlight the ability of AuNP-PADRE^S2P6 peptide conjugates to elicit antibody production of relevant specificity against the SARS-CoV-2 spike protein.
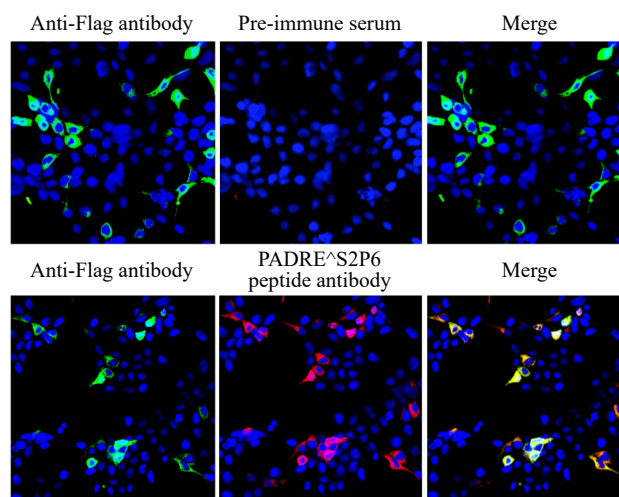

Figure 6. RRecognition of Omicron spike protein by PADRE^S2P6 peptide-reactive antibody. HEK-293T cells transfected 24 h with pcDNA3/rS expressing the recombinant spike protein from SARS-CoV-2 Omicron variant were co-labelled with a rabbit anti-FLAG antibody at dilution 1:500 and mouse immune serum raised against AuNP-PADRE^S2P6 peptide conjugates (PADRE^S2P6 peptide antibody) at dilution 1:100. The respective pre-immune serum served as negative serum control. Donkey IgG anti-rabbit IgG-Alexa Fluor 488 and anti-mouse IgG-Alexa Fluor 594 were used as secondary antibodies. Nuclei were stained by DAPI. Slides were observed under 20x lens magnification.

4. Conclusions

Over the last decades, there was a significant effort made in the development of AuNP-based assays for pathogen detection [16, 17]. To date, COVID-19 pandemic still remains a challenging public health with the global spread of SARS-CoV-2 and rapid emergence of highly contagious variants such as Omicron which rapidly became the dominant VOC in many countries. The development of tools for laboratory-based serological detection of SARS-CoV-2 contributes to the global fight against pandemic COVID-19. In the present study, we investigated whether peptide-conjugated AuNPs could be considered as an innovative approach for SARS-CoV-2 detection with the production of specific reactive antibodies against the spike protein. We recently reported that the synthetic S1P4 and S2P6 peptides representing SARS-CoV-2 spike residues 616/644 and 1138/1169, respectively were recognized by the immune sera from COVID-19 mRNA BNT162 vaccine (brand name Comirnaty vaccine purchased by Pfizer/BioNTech). The synthetic S2P6 peptide and to lesser extent the synthetic S1P4 peptide, were immunogenic as protein-peptide conjugates in BALB/c mice [4].

Research on nanoparticles has focused on the development of new strategies for synthetizing AuNPs such as a green chemistry approach resulting in greater stability and lower toxicity in vivo [13]. It has been established that AuNPs injected in a tissue can be captured by professional antigen-presenting cells (APCs) mostly lymph node-resident dendritic cells (LN-resident DCs) [18, 19]. The inherent capacity of AuNPs to target APCs may be of a great interest to initiate an antigen-specific immune response resulting in the activation of humoral immunity. This prompted us to evaluate whether AuNPs obtained by an environmental-friendly process and functionalized with synthetic peptides are efficient to elicit a specific antibody response against SARS-CoV-2. In the present study, the synthetic PADRE^S1P4 and PADRE^S2P6 peptides were designed to include SARS-CoV-2 antibody epitope preceded by the T-helper cell response activator PADRE and a polybasic sequence leading to a potential release of immobilized peptide from nanoparticle surface. The synthetic PADRE^S1P4 and PADRE^S2P6 peptides were conjugated to AuNPs and immunogenicity of nanoconjugates were assessed in adult BALB/c mice. The animals were inoculated intramuscularly with three low doses of AuNP-peptide conjugates in a prime-boost schedule. Mice that received repeated doses of functionalized AuNPs by intramuscular route did not shown morbidity suggesting that AuNP-peptide conjugates are not inherently toxic to animals.

Inoculation of adult BALB/c mice with AuNP-PADRE^S2P6 peptide conjugates was efficient to generate a significant production of specific antibodies that are reactive with SARS-CoV-2 spike protein. The fact that intramuscular administration AuNP-PADRE^S2P6 peptide conjugates induced humoral response without the need for adjuvant may suggest a direct traffic of nanoconjugates towards the LN-resident DCs to initiate humoral response [18, 19]. There was no specific antibody response in BALB/c mice that received the AuNP-PADRE^S1P4 peptide conjugates. We cannot exclude that incapacity of such nanoconjugates to elicit humoral immunity was a direct consequence of the lower immunogenicity of the S1P4 peptide compared to the S2P6 peptide [4]. The inefficiency of AuNP-PADRE^S1P4 peptide conjugates could also relate to a defect in orientation of PEGylated PADRE^S1P4 peptide at the AuNP surface due to the presence of a free sulfhydryl group in the Cys23 residue of the S1P4 peptide.

Remarkably, the PADRE^S2P6 peptide-reactive antibodies can recognize dominant SARS-CoV-2 Omicron variant suggesting that AuNP-peptide conjugates should be considered as promising laboratory-adapted tools for immune detection of live virus as well as SARS-CoV-2 spike protein. Due to their photo-optical distinctiveness and biocompatibility, AuNPs are described as promising tools for biosensing applications [20, 21]. Given that linear B-cell epitope namely S2P6 is a feature of recombinant spike protein expressed by COVID-19 mRNA BNT162 vaccine (trademark Comirnaty by Pfizer-BioNTech), another interesting perspective of this study would be to evaluate the potential application of AuNP-PADRE^S2P6 peptide conjugates for antibody monitoring in Comirnaty vaccine recipients.

In conclusion, our study demonstrated that eco-friendly manufactured AuNPs functionalized with the synthetic PADRE^S2P6 peptide representing a conserved linear B-cell epitopes of SARS-CoV-2 spike protein are suitable for production of antibodies of relevant specificity without the need for potentially harmful adjuvants. Accordingly generated PADRE^S2P6 peptide-reactive antibodies can recognize all tested SARS-CoV-2 variants. Now positioning of such peptide-reactive antibodies in COVID-19 diagnostic strategies remains to be investigated. Considering the likelihood of new outbreaks associated with emerging zoonotic pathogens [22], application of viral peptide-conjugated AuNPs for surveillance of wildlife-origin coronaviruses identified as potential source of infectious diseases of medical
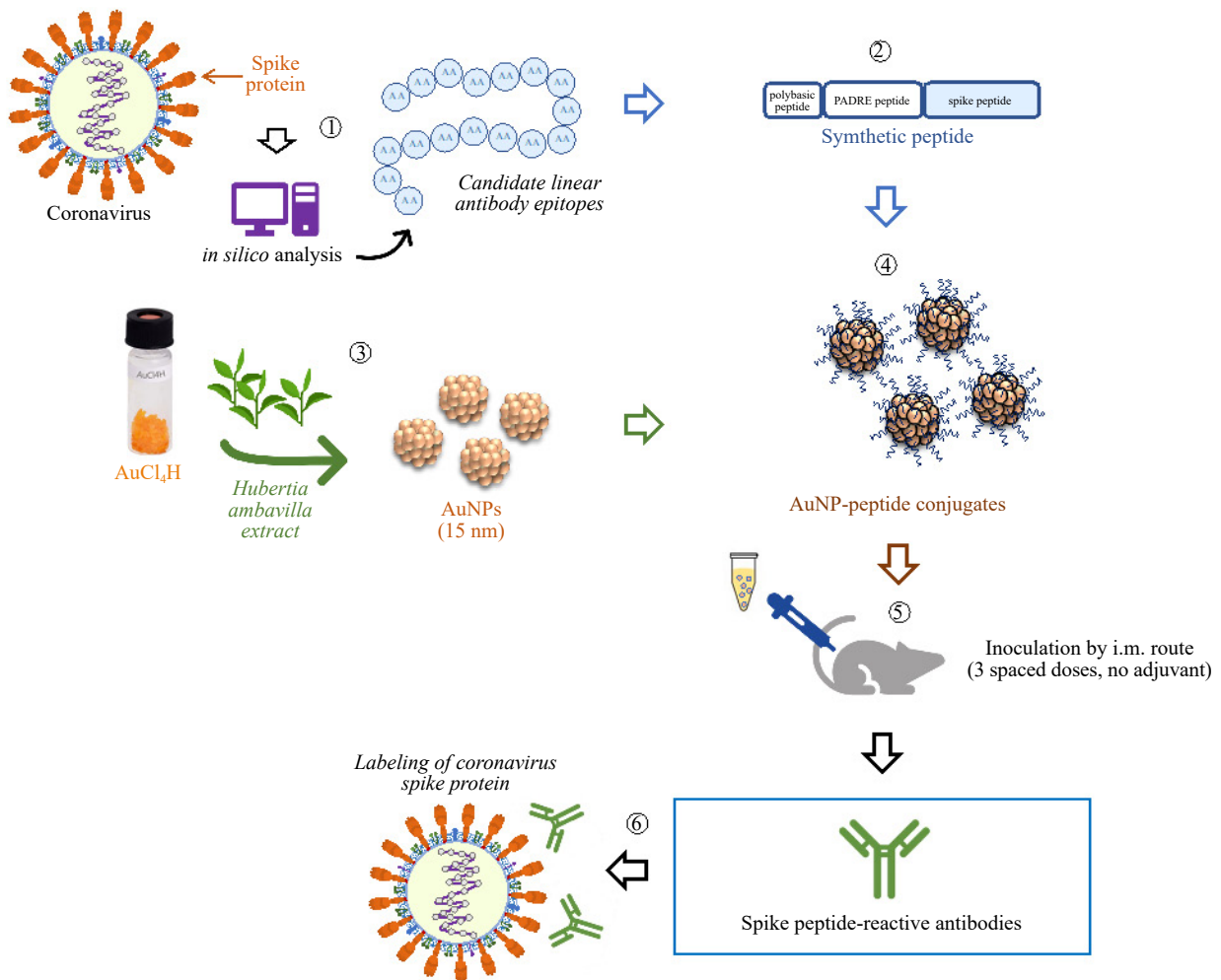
concern is a promising strategy (Figure 7) [15, 19].

Figure 7. Flow chart for preparation of coronavirus spike protein-reactive antibodies based on AuNP-peptide conjugates. *In* (1), *in silico* prediction of linear B-cell epitopes (antibody epitopes) on coronavirus spike protein. *In* (2), production of a synthetic peptide corresponding to candidate spike antibody epitope preceded by immune modulator PADRE and a polybasic sequence. *In* (3) AuNPs can be prepared by an environmental-friendly process using plant extracts (12). *In* (4), AuNPs are functionalized by using a PEG-SH substrate linked to the first amino-acid of synthetic peptide. *In* (5), administration of AuNP-peptide conjugates in PBS by intra-muscular route without the need for adjuvants in a prime-boost schedule. Animals are bled few weeks after the last inoculation. *In* (6), immune sera are assessed for reactivity of anti-peptide antibody against coronavirus spike protein.

Acknowledgments

Conflict of interest

There is no conflict of interest for this study.There is no conflict of interest for this study.
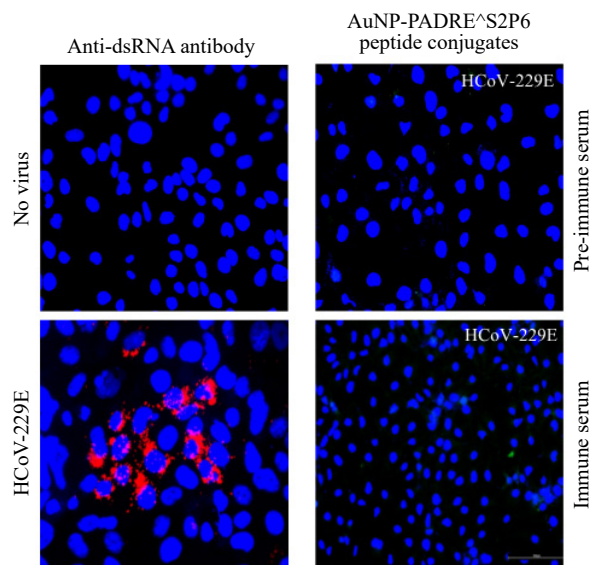
Appendix

Figure A1. Immune reactivity against HCoV-229E virus. IF analysis on Huh 7.5 cells infected 24 h by alphacoronavirus HCoV-229E or mock-infected (no virus). In left, HCoV-229E virus replication in Huh7 cells was verified using mouse anti-dsRNA J2 monoclonal antibody as primary antibody. In right, virus-infected cells (HcoV-229E) were assessed with immune serum raised against AuNP-PADRE^S2P6 peptide conjugates or pre-immune serum at dilution 1:100. Donkey IgG anti-mouse IgG-Alexa Fluor 594 was used as secondary antibody. Nuclei were stained by DAPI. Slides were observed under 20x lens magnification.
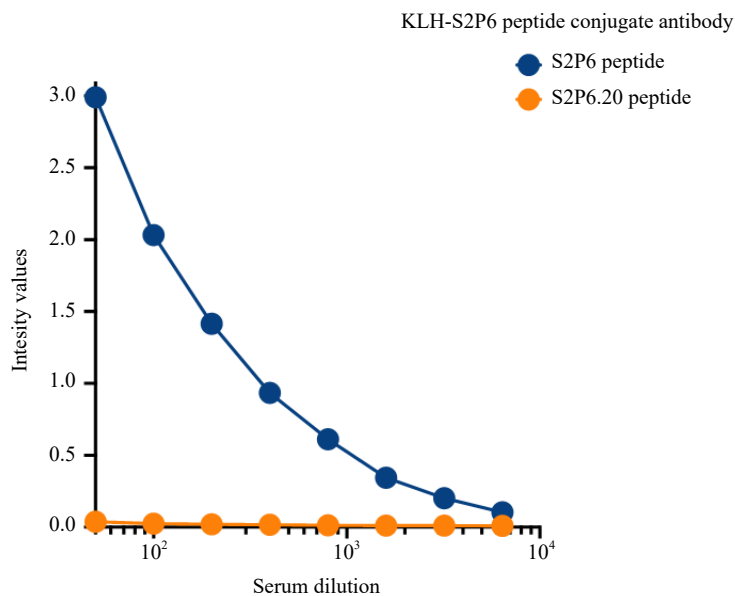

Figure A2. Dose-response curve of serum sample from a mouse immunized with KLH-S2P6 peptide conjugates in a prime-boost schedule. The peptide-based ELISA was performed using synthetic S2P6 peptide. The synthetic S2P6.2.0 peptide served as negative peptide control. The intensity values of serum samples were measured at OD_{450}.

References

[1]   Ellwanger JH, Chies JAB. Zoonotic spillover: Understanding basic aspects for better prevention. *Genetics and Molecular Biology*. 2021; 44: e20200355. Available from: https://doi.org/10.1590/1678-4685-gmb-2020-0355.

[2]   Hu B, Guo H, Zhou P, Shi ZL. Characteristics of SARS-CoV-2 and COVID-19. *Nature Reviews Microbiology*. 2021;19(3):141-154. Available from: https://doi.org/10.1038/s41579-020-00459-7.

[3]   Msemburi W, Karlinsky A, Knutson V, Aleshin-Guendel S, Chatterji S, Wakefield J. The WHO estimates of excess mortality associated with the COVID-19 pandemic. *Nature*. 2022; 613: 130–137. Available from: https://doi.org/10.1038/s41586-022-05522-2.

[4]   Andries J, Viranaicken W, Cordonin C, Herrscher C, Planesse C, Roquebert B, Lagrange-Xelot M, El-Kalamouni C, Meilhac O, Mavingui P, Couret D. The SARS-CoV-2 spike residues 616/644 and 1138/1169 delineate two antibody epitopes in COVID-19 mRNA COMIRNATY vaccine (Pfizer/BioNTech). Scientific Reports. 2022; 12(1): 5999. Available from: https://doi.org/10.1038/s41598-022-10057-7.

[5]   Pati R, Shevtsov M, Sonawane A. Nanoparticle vaccines against infectious diseases. Frontiers in immunology. 2018; 9: 2224. Available from: https://doi.org/10.3389/fimmu.2018.02224.

[6]   Tregoning JS, Flight KE, Higham SL, Wang Z, Pierce BF. Progress of the COVID-19 vaccine effort: viruses, vaccines and variants versus efficacy, effectiveness and escape. *Nature reviews immunology*. 2021; 21(10): 626-636. Available from: https://doi.org/10.1038/s41577-021-00592-1.

[7]   Vu MN, Kelly HG, Kent SJ, Wheatley AK. Current and future nanoparticle vaccines for COVID-19. *eBioMedicine*. 2021; 74: 103699. Available from: https://doi.org/10.1016/j.ebiom.2021.103699.

[8]   Kyriakidis NC, López-Cortés A, González EV, Grimaldos AB, Prado EO. SARS-CoV-2 vaccines strategies: a comprehensive review of phase 3 candidates. *npj Vaccines*. 2021; 6(1): 28. Available from: https://doi.org/10.1038/s41541-021-00292-w.

[9]   Dykman LA. Gold nanoparticles for preparation of antibodies and vaccines against infectious diseases. *Expert review of vaccines*. 2020; 19(5): 465-477. Available from: https://doi.org/10.1080/14760584.2020.1758070.

[10]   Carabineiro SAC. Applications of Gold Nanoparticles in Nanomedicine: Recent Advances in Vaccines. *Molecules*. 2017; 22(5): 857. Available from: https://doi.org/10.3390/molecules22050857.

[11]   Enea M, Pereira E, Peixoto de Almeida M, Araújo AM, Bastos MD, Carmo H. Gold nanoparticles induce oxidative stress and apoptosis in human kidney cells. *Nanomaterials*. 2020; 10(5): 995. Available from: https://doi.org/10.3390/nano10050995.

[12]   Morel AL, Giraud S, Bialecki A, Moustaoui H, de La Chapelle ML, Spadavecchia J. Green extraction of endemic plants to synthesize gold nanoparticles for theranostic applications. *Frontiers in Laboratory Medicine*. 2017; 1(3): 158–171. Available from: https://doi.org/10.1016/j.flm.2017.10.003.

[13]   Haddada MB, Gerometta E, Bialecki A, Fu W, Zhang Y, de La Chapelle ML, Djaker N, Pesnel S, Morel AL, Spadavecchia J. Endemic plants: From design to a new way of smart hybrid nanomaterials for green nanomedicine applications. *Journal of Nanomedicine & Nanotechnology*. 2018; 9: 518. Available from: https://doi.org/10.4172/2157-7439.1000518.

[14]   Haddada MB, Aouidat F, Monteil M, Lecouvey M, de la Chapelle ML, Spadavecchia J. A simple assay for direct colorimetric detection of prostatic acid phosphatase (PAP) at fg levels using biphosphonated loaded PEGylated gold nanoparticles. *Frontiers in Laboratory Medicine*. 2017; 1(4): 186–191. Available from: https://doi.org/10.1016/j.flm.2017.11.005.

[15]   Fagúndez, P.; Botasini, S.; Tosar, J.P.; Méndez, E. Systematic process evaluation of the conjugation of proteins to gold nanoparticles. *Heliyon*. 2021; 7(6): e07392. Available from: https://doi.org/10.1016/j.heliyon.2021.e07392.

[16]   Wang J, Drelich AJ, Hopkins CM, Mecozzi S, Li L, Kwon G, Hong S. Gold nanoparticles in virus detection: Recent advances and potential considerations for SARS-CoV-2 testing development. *WIREs: Nanomedicine and Nanobiotechnology*. 2022; 14(1): e1754. Available from: https://doi.org/10.1002/wnan.1754.

[17]   Draz MS, Shafiee H. Applications of gold nanoparticles in virus detection. *Theranostics*. 2018; 8(7): 1985-2017. Available from: https://doi.org/10.7150/thno.23856.

[18]   Patel S, Kim J, Herrera M, Mukherjee A, Kabanov AV, Sahay G. Brief update on endocytosis of nanomedicines. *Advanced Drug Delivery Reviews*. 2019; 144: 90-111. Available from: https://doi.org/10.1016/j.addr.2019.08.004.

[19]   Manolova V, Flace A, Bauer M, Schwarz K, Saudan P, Bachmann MF. Nanoparticles target distinct dendritic cell populations according to their size. *European Journal of Immunology*. 2008; 38(5): 1404-1413. Available from: https://doi.org/10.1002/eji.200737984.

[20]   Zhou W, Gao X, Liu D, Chen X. Gold nanoparticles for in vitro diagnostics. *Chemical Reviews*. 2015; 115(19): 10575–10636. Available from: https://doi.org/10.1021/acs.chemrev.5b00100.

[21] Baptista P, Pereira E, Eaton P, Doria G, Miranda A, Gomes I, Quaresma P, Franco R. Gold nanoparticles for the development of clinical diagnosis methods. *Analytical and Bioanalytical Chemistry*. 2008; 391: 943–950. Available from: https://doi.org/10.1007/s00216-007-1768-z.

[22] Bloom DE, Black S, Rappuoli R. Emerging infectious diseases: A proactive approach. *Proceedings of the National Academy of Sciences*. 2017; 114(16): 4055–4059. Available from: https://doi.org/10.1073/pnas.1701410114.